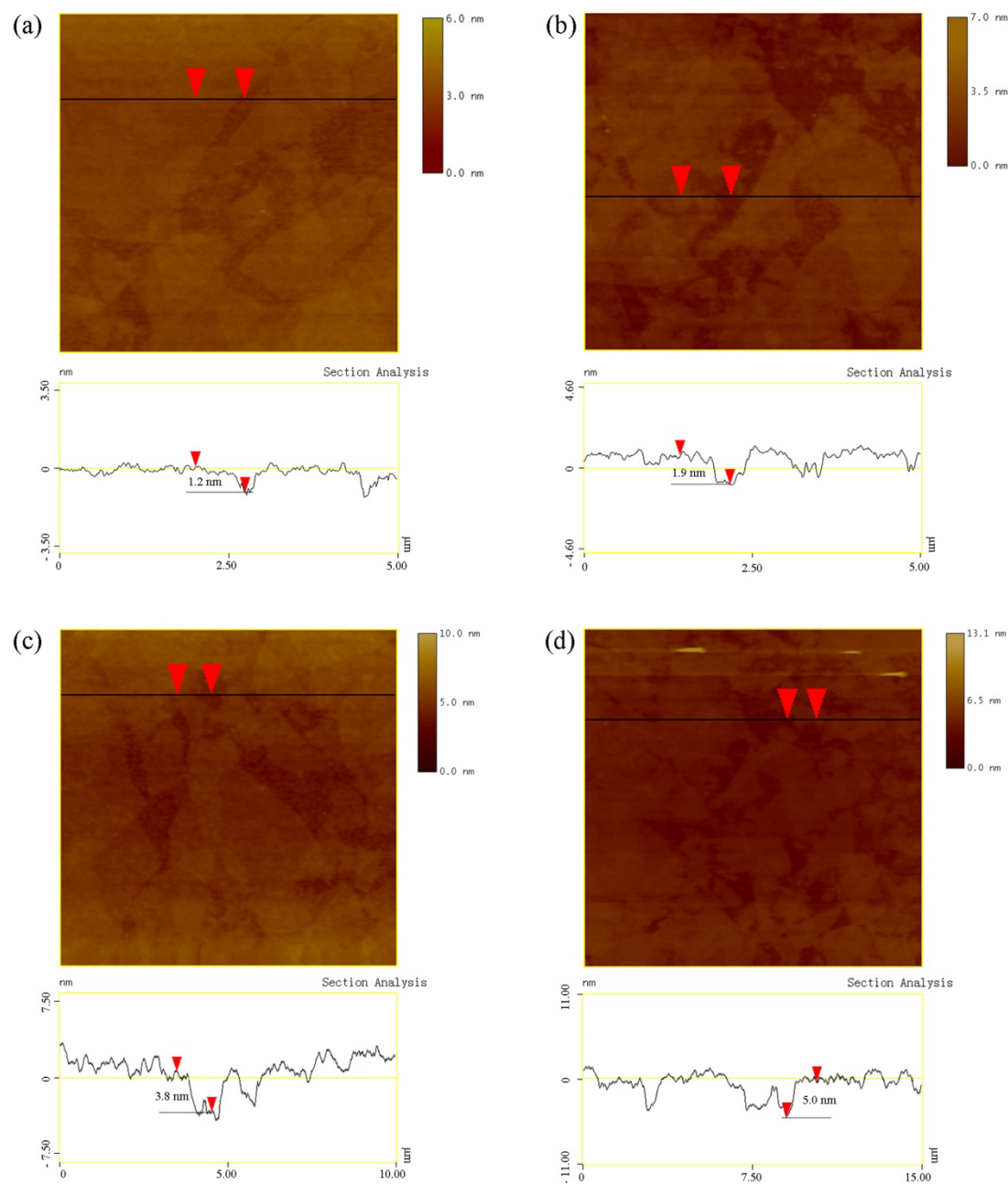
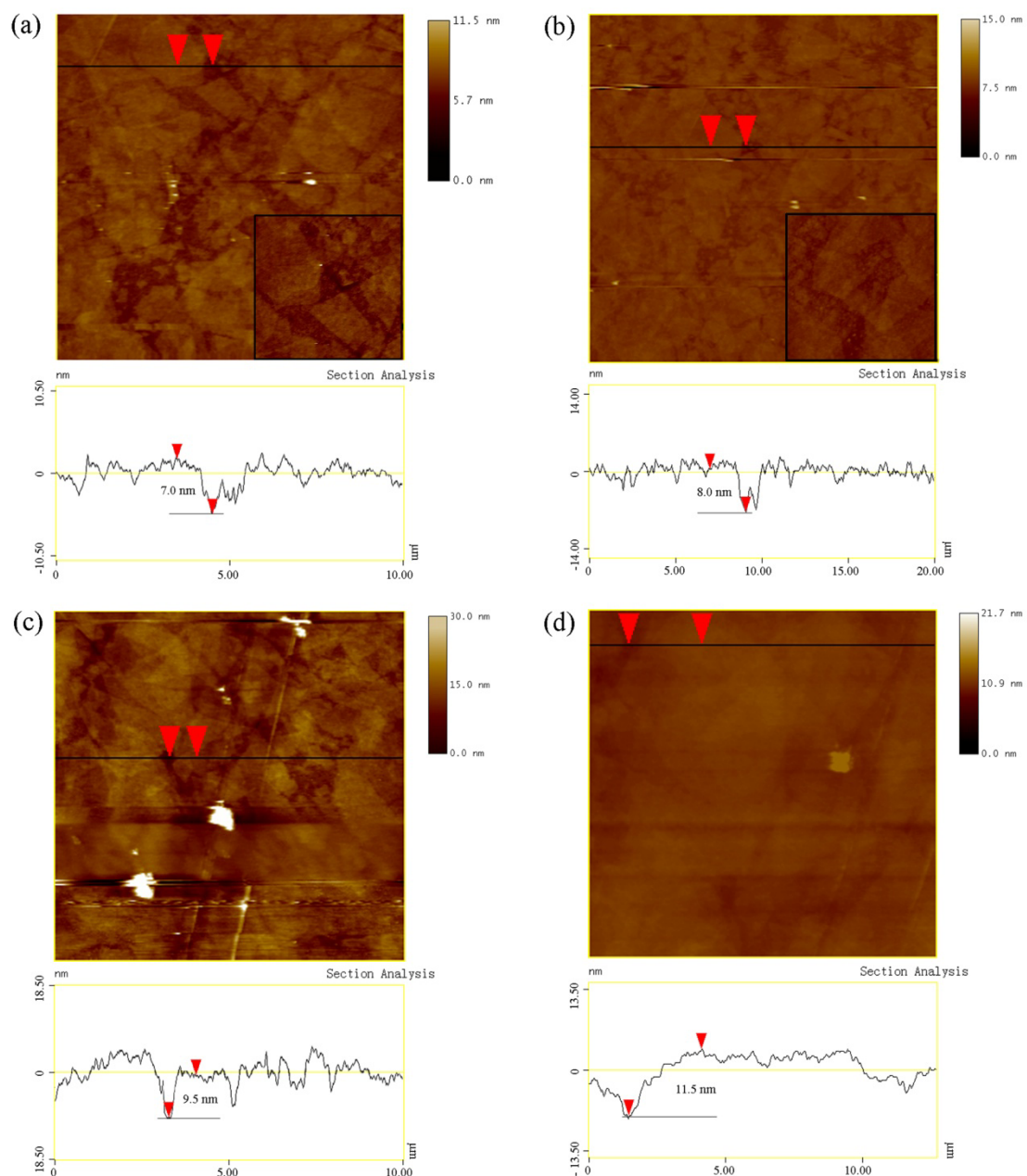


## Supporting information

### 1. Taping mode section analys in CTR-GE films with different initial filtering concentrations



**Fig. S1** AFM image and taping mode section analysis on CTR-GE films with different initial filtering concentrations; (a)  $19 \text{ mg L}^{-1}$ , (b)  $58 \text{ mg L}^{-1}$ , (c)  $92 \text{ mg L}^{-1}$  and (d)  $107 \text{ mg L}^{-1}$ . AFM images were captured with CTR-GE/SiO<sub>2</sub>/Si samples.



**Fig. S2** AFM image and taping mode section analysis on CTR-GE films with different initial filtering concentrations; (a)  $125 \text{ mg L}^{-1}$ , (b)  $139 \text{ mg L}^{-1}$ , (c)  $149 \text{ mg L}^{-1}$  and (d)  $168 \text{ mg L}^{-1}$ . AFM images were captured with CTR-GE/SiO<sub>2</sub>/Si samples. Insets of (a) and (b) are the magnified images of these films (in  $1\mu\text{m}\times 1\mu\text{m}$  field).

Fig. S1 and Fig. S2 show the AFM image and taping mode section analysis in CTR-GE films that were obtained from different initial filtering concentrations and equal filtering volume (1mL) of CR-GE dispersion. Taping mode analysis results suggest that film thickness is gradually increased with the increasing filtering concentration.

## 2. Sheet resistance and transmittance list for different samples.

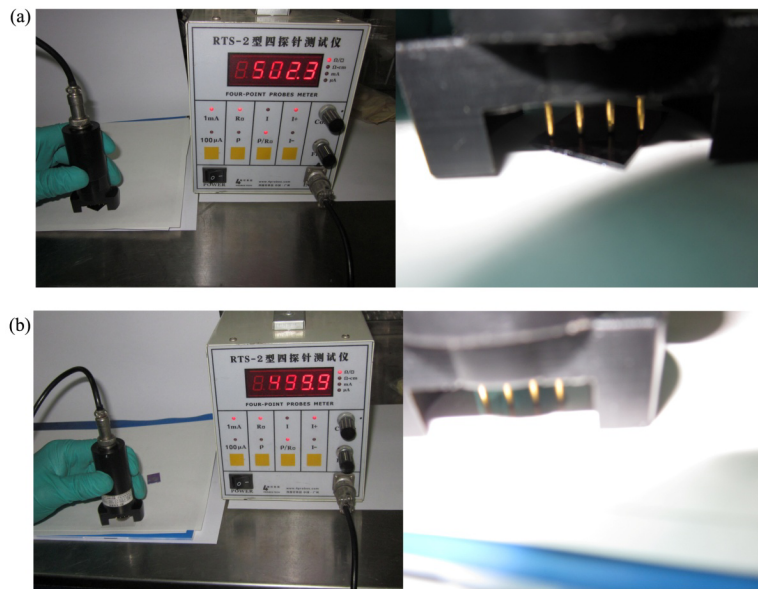


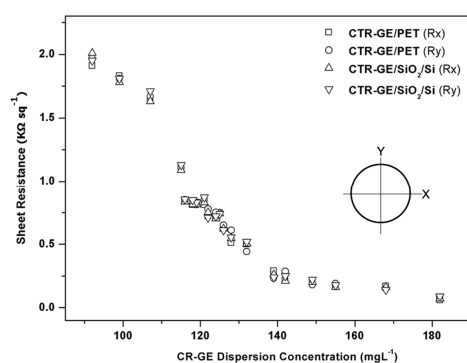
**Fig. S3** Photographs of measuring sheet resistances by Resistance Meter (RTS-2) (left) and magnitude image for contact points of four-point-probe head with the samples (right). (a) CTR-GE/SiO<sub>2</sub>/Si sample. (b) Flexible CTR-GE/PET sample. CTR-GE films on both of PET and SiO<sub>2</sub>/Si substrates were produced from the same initial filtering concentration (132mg L<sup>-1</sup>).

Since the film thickness of CTR-GE films on PET substrates could not directly observe by AFM, we investigated the sheet resistance of CTR-GE/SiO<sub>2</sub>/Si and CTR-GE /PET films indirectly representing the thickness information of the films. The free-standing CTR-GE films with the same initial filtering concentration were transferred to SiO<sub>2</sub>/Si flakes and flexible PET films. The sheet resistances were measured by Resistance Meter (RTS-2) using a four-point-probe head with a pin-distance of about 4 mm (see Fig. S3). The conducting paste was not used during the measurement process. The sheet resistances were measured along the vertical cross lines ("X", "Y") in each sample. The four-point-probe head is contacted with the whole diameter scale of flexible CTR-GE/PET sample. Therefore, it could represent the whole area of the flexible CTR-GE/PET samples. The measure results are shown in table 1.

**Table 1** Sheet resistance and transmittance list for different samples.

| C<br>(mg L <sup>-1</sup> ) | CR-GE/PET        |                         |       | CTR-GE/PET       |                         |       | CTR-GE/SiO <sub>2</sub> /Si |       |
|----------------------------|------------------|-------------------------|-------|------------------|-------------------------|-------|-----------------------------|-------|
|                            | Flexible Films   |                         |       | Flexible Films   |                         |       | Flakes                      |       |
|                            | T (%)<br>(550nm) | R (KΩsq <sup>-1</sup> ) |       | T (%)<br>(550nm) | R (KΩsq <sup>-1</sup> ) |       | Rx                          | Ry    |
|                            |                  | Rx                      | Ry    |                  | Rx                      | Ry    |                             |       |
| 182                        | 47.7             | 1.3                     | 1.5   | 38.5             | 0.06                    | 0.08  | 0.07                        | 0.09  |
| 168                        | 56.8             | 2.6                     | 1.8   | 51.2             | 0.17                    | 0.15  | 0.16                        | 0.14  |
| 155                        | 64.88            | 2.9                     | 2.91  | 60.38            | 0.17                    | 0.19  | 0.162                       | 0.178 |
| 149                        | 67.8             | 3.3                     | 2.76  | 63.8             | 0.2                     | 0.18  | 0.2                         | 0.22  |
| 142                        | 72.54            | 3.9                     | 4.22  | 68.08            | 0.215                   | 0.285 | 0.21                        | 0.25  |
| 139                        | 73.4             | 3.52                    | 4.32  | 69.5             | 0.29                    | 0.232 | 0.261                       | 0.239 |
| 132                        | 77.68            | 5.3                     | 4.9   | 75.15            | 0.499                   | 0.441 | 0.502                       | 0.52  |
| 128                        | 80.57            | 6.2                     | 6.06  | 76.35            | 0.51                    | 0.61  | 0.545                       | 0.555 |
| 126                        | 81.33            | 6.5                     | 6.18  | 79.4             | 0.63                    | 0.65  | 0.62                        | 0.61  |
| 125                        | 82.3             | 8.3                     | 7.9   | 79.5             | 0.745                   | 0.741 | 0.74                        | 0.739 |
| 124                        | 82.9             | 9.56                    | 9.64  | 79.58            | 0.71                    | 0.75  | 0.70                        | 0.72  |
| 122                        | 83.6             | 10.5                    | 10.1  | 79.73            | 0.723                   | 0.777 | 0.75                        | 0.71  |
| 121                        | 84.2             | 11.5                    | 11.4  | 79.97            | 0.81                    | 0.85  | 0.83                        | 0.87  |
| 119                        | 84.9             | 12.8                    | 11.5  | 80.02            | 0.83                    | 0.81  | 0.812                       | 0.828 |
| 118                        | 85.2             | 11.9                    | 13.3  | 80.07            | 0.81                    | 0.83  | 0.812                       | 0.848 |
| 116                        | 85.7             | 12.9                    | 14.1  | 80.23            | 0.845                   | 0.85  | 0.835                       | 0.842 |
| 115                        | 86.1             | 14.2                    | 13.6  | 83.23            | 1.12                    | 1.11  | 1.09                        | 1.13  |
| 107                        | 89.1             | 45.9                    | 48.3  | 87.6             | 1.65                    | 1.67  | 1.63                        | 1.71  |
| 99                         | 90.8             | 67.7                    | 71.7  | 89.1             | 1.83                    | 1.81  | 1.78                        | 1.81  |
| 92                         | 91.8             | 81.2                    | 79.4  | 89.9             | 1.91                    | 1.97  | 2.01                        | 1.95  |
| 58                         | 95.0             | 122.3                   | 120.5 | 93.7             | 33.2                    | 33.3  | 31.8                        | 32.3  |
| 19                         | 97.5             | 158.8                   | 159.7 | 97.2             | 70.4                    | 70.3  | 69.6                        | 71.3  |

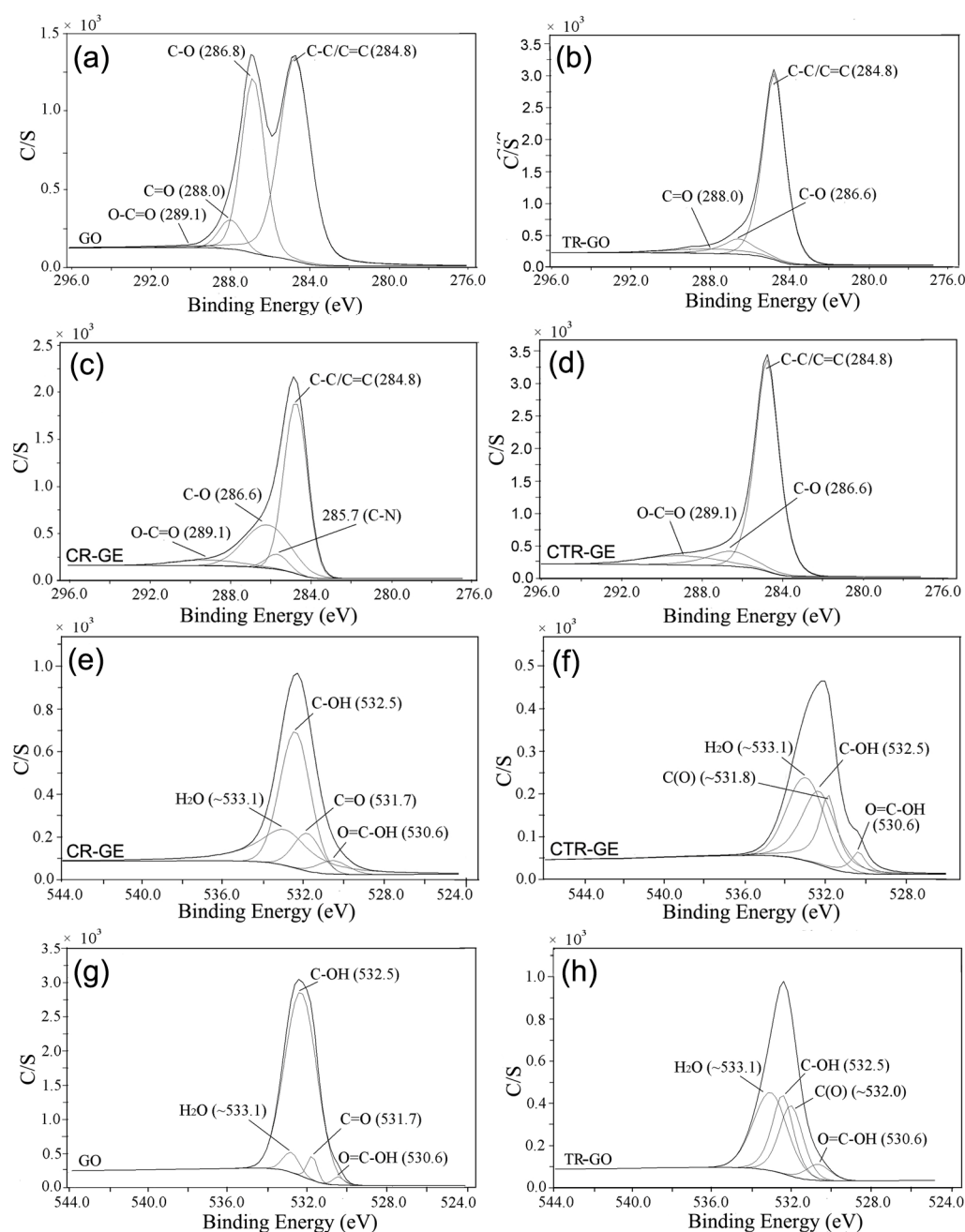
● “Rx” and “Ry”: Sheet resistance for vertical cross lines (X and Y) in each sample.



**Fig. S4.** Comparison of sheet resistances between CTR-GE/SiO<sub>2</sub>/Si film and CTR-GE/PET films. Sheet resistances were measured along the vertical cross lines in each sample.

In Table.1, “C” indicates the initial filtering concentrations of CR-GE dispersion. “T” indicates the transmittances of the transparent samples at irradiation wavelength of 550 nm, and the listed T% is the average values of ten different measure points in each sample. Sheet resistances were measured along the vertical cross lines (“X”, “Y”) in each sample. Based on the measuring results listed in Table.1, we compared the sheet resistances between CTR-GE/PET and CTR-GE/ SiO<sub>2</sub>/Si. Each pair of CTR-GE/PET and CTR-GE/ SiO<sub>2</sub>/Si samples is corresponded to the same initial filtering concentrations. This result is shown in Fig. S4. As shown in Fig.S4, the sheet resistance values of the CTR-GE/PET samples are approximate to the values of CTR-GE/SiO<sub>2</sub>/Si in each pair samples, indirectly suggesting that CTR-GE/SiO<sub>2</sub>/Si film and CTR-GE/PET have the same structural and thickness information.

### 3. XPS analysis



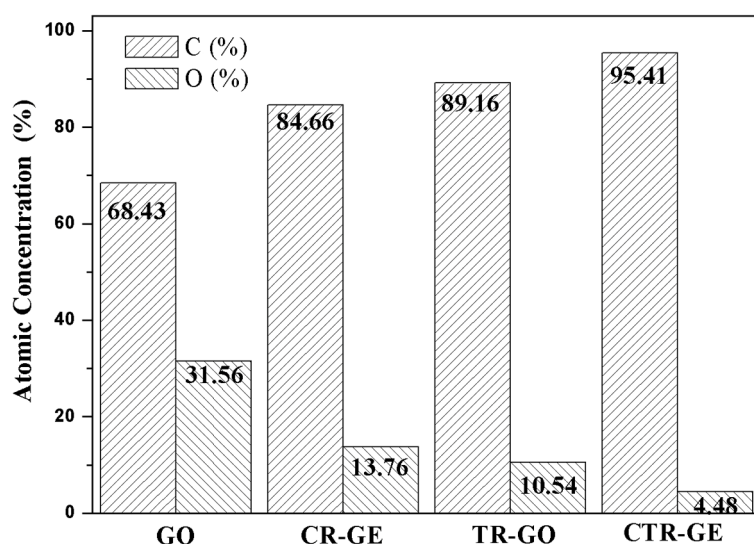
**Fig. S5** High-resolution XPS analysis for GO, CR-GE, TR-GO and CTR-GE films. (a)-(d) C1s spectra for GO, CR-GE, TR-GO, CTR-GE films. (e)-(h) O1s spectra for GO, CR-GE, TR-GO, CTR-GE films. Relative intensities of peaks are shown by the scale areas for axis of C/S.

Fig. S5 shows high-resolution XPS spectra for GO, CR-GE, TR-GO and CTR-GE samples. SDP Ver. 4.0 software was utilized to analyze and deconvolute the XPS peaks. In Fig 6S, peak deconvolutions were performed using Gaussian components after a Shirley background subtraction. The oxygen-containing functional groups were introduced to GO in the form of C-O (hydroxyl/epoxy, 286.8 eV), C=O (carbonyl, 288.0 eV) and O-C=O (carboxyl, 289.1 eV) (Fig 5Sa). As shown in Fig 5Sd, hydroxyl/epoxy groups were reduced significantly and the C-C/C=C (284.8 eV) sp<sup>2</sup> domains were restored obviously in CTR-GE sample. The C-N signal (285.7 eV) appears in CR-GE,

suggesting the formation of hydrazine-related groups during the chemical reduction process with hydrazine hydrate (Fig 5Sc). O1s spectra consist of multiple peaks located at 532.5eV (C-OH), 530.6eV (O=C-OH), 533.1eV (H<sub>2</sub>O), 531.7eV(C=O), and the relative intensities of peaks are shown by the scale areas for axis of C/S, verifying significant reduction of the oxygen-containing functional groups in CTR-GE sample. The efficient deoxygenation by both reduction processes of excess amount hydrazine-reduction and further thermal reduction is also obvious in O1s spectra for CTR-GE sample (Fig 5Sf).

**Table 2 Element compositions in samples (%)**

| Samples | C1s (%)<br>[0.314] | O1s (%)<br>[0.733] | N1s (%)<br>[0.499] | Si2s (%)<br>[0.347] | Si2p (%)<br>[0.368] | Al2p (%)<br>[0.256] |
|---------|--------------------|--------------------|--------------------|---------------------|---------------------|---------------------|
| CTR-GE  | 95.41              | 4.48               | -                  | 0.03                | 0.08                | -                   |
| TR-GO   | 89.16              | 10.54              | -                  | 0.10                | 0.20                | -                   |
| CR-GE   | 84.66              | 13.76              | 1.58               | -                   | -                   | -                   |
| GO      | 68.43              | 31.56              | -                  | -                   | -                   | -                   |



**Fig.S6** A bar graph summary of element (C and O) compositions in each sample.

Fig. S6 shows the element (C and O) composition results in each sample. C/O ration values in typical previous results and element composition analysis example are shown in below two tables. In comparison with the results in below two tables, our result shows improved graphitization in CTR-GE sample.

#### 4. Direct structural Information

Because direct structural characterizations including XRD, Raman, *etc.* on CTR-GE/PET samples were affected the influence of the plastic substrate (PET), we didn't provide the measurement information (XRD, Raman) for CTR-GE/PET samples.

According to reviewer(s)' comments we provide these measure results.

- XRD measure result on CTR-GE/PET sample

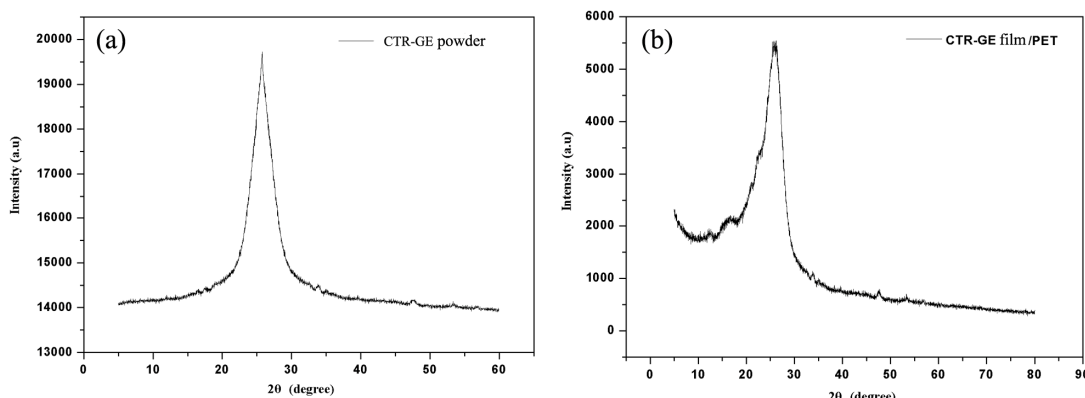


**Fig. S7.** XRD spectra of CTR-GE samples: (a) grinded free-standing CTR-GE sample; (b) FTGF sample (on PET substrate)

Shown in Fig.S7 are the XRD spectra of the CTR-GE samples Fig. S7a is the grinded free-standing CTR-GE sample and Fig. S7b is the FTGF sample. The results show that the CTR-GE and FTGF sample have the same structure except for the difference of the peak shapes, which result from the effect of the PET.

Raman measure result on CTR-GE/PET sample

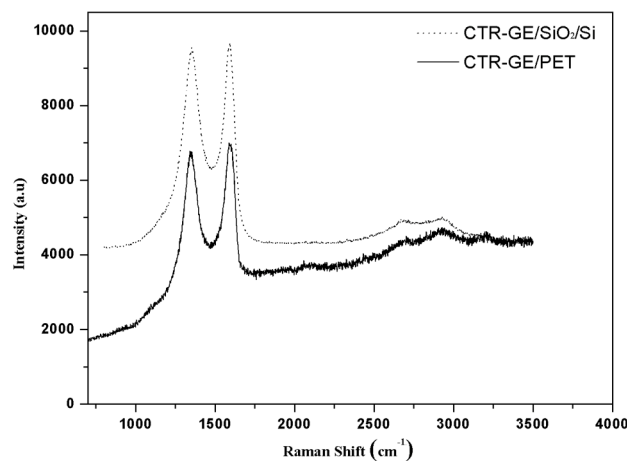


**Fig. S8.** Raman spectra of CTR-GF transferred on SiO<sub>2</sub>/Si and PET substrates.

Fig.S8 are the Raman spectra of CTR-GF transferred on SiO<sub>2</sub>/Si and PET substrates, showing that the structural information of the FTGF is the same as that of the CTR-GE/ SiO<sub>2</sub>/Si except for the high background intensity which result from the effect of the PET. The Raman results revealed that the CTR-GE/ SiO<sub>2</sub>/Si sample have the same structural information as the FTGFs sample.